# Low-Frequency Oscillations of the Large-Scale Stratospheric Temperature Field

XIN HAI GAO AND JOHN L. STANFORD

*Physics Department, Iowa State University, Ames, IA 50011*

(Manuscript received 11 February 1986, in final form 23 January 1987)

ABSTRACT

Low-frequency analyses are reported for four years of 3-day-mean satellite microwave and infrared data representative of temperatures in the stratosphere. In data representative of 30–150 mb temperatures, oscillations with 39–51 day periods are observed as a tropical dipole pattern in the Indonesia/central Pacific. In addition, the first evidence is presented for such oscillations in the southeast Pacific. Furthermore, significant 39–51 day oscillations are observed in the mid- and upper stratosphere, centered near 60°S latitude.

## 1. Introduction

Since Madden and Julian (1971) first reported a 40–50 day oscillation in 10 years of rawinsonde data for Canton Island (3°S, 172°W), many other observations have confirmed these low-frequency oscillations in the tropical troposphere. Several recent investigators have suggested that the frequency band of these low-frequency oscillations may be quite broad. Murakami et al. (1984) showed that the convective activity over the western Pacific varied with a period of 30–40 days and was closely associated with that of the Asian monsoon. Weickmann (1982, 1983) investigated intraseasonal fluctuations in OLR (outgoing longwave radiation) data, and Weickmann et al. (1985) have more recently studied the 30–60 day spectral band for 10 Northern Hemisphere (NH) winters of OLR data and noted that the OLR variance at periods between 28 and 72 days is large over the equatorial Indian Ocean, the maritime continent of Indonesia, and South America. Lau and Chan (1985) also studied the 40–50 day oscillation in the OLR time series for the tropics and suggested that these oscillations may be related to extratropical OLR anomalies. Quah (1984) reported that the 30–50 day mode oscillation was observed in some extratropical areas.

In addition to these observational analyses, a number of modeling studies have been done on the low-frequency oscillations. Chang (1977) attempted to explain them by examining Kelvin waves in the tropics, including cumulus cloud drag and radiative damping. But the dispersion relation was found to be perhaps too sensitive to the value of the damping coefficients. Moreover, this model would presumably be seasonally dependent, through Doppler shifting by the zonal mean wind. However, little seasonality could be detected in an observational study of 25 years of rawinsonde data for Truk Island (Anderson et al., 1984). Yamagata and Hayashi (1984) studied the response of the equatorial atmosphere to a heating source oscillating with a 40 day period. Their simplified shallow water model showed that the main features of the observed nonsymmetric components of the oscillation can be explained if the heating is located over the maritime continent. However, the reason for the periodicity of the heating was not explained. Anderson and Stevens (1987) advanced the hypothesis that the low frequency oscillations result from the advective time scale associated with a Hadley basic state circulation. Webster (1983) suggested that surface hydrological effects could result in monsoon variations of 40–50 day time scale, and similar oscillations in a zonally symmetric general circulation model have been discussed by Goswami and Shukla (1984).

Although the presence of the low frequency oscillations in the tropics have been confirmed for some time by a number of observational papers, and although related modeling studies have been done, many aspects of these oscillations remain to be fully understood. Among the questions still unanswered is the extent to which such oscillations, or influences due to them, occur in the middle and high latitudes, and in higher altitude levels.

With this question in mind we analyze four years of globally gridded, satellite-derived brightness temperature data from polar-orbiting satellites. Four different channels (MSU4, SSU1, SSU2, SSU3) sensitive to atmospheric temperatures near 90, 15, 5 and 1.5 mb, respectively, were used.

## 2. Data and analyses

In this study, four years of MSU4 (Microwave Sounding Unit channel 4) and SSU (Stratospheric Sounding Unit) data have been used to investigate the low frequency oscillations in the stratosphere. The MSU4 measures the magnetic dipole radiation of molecular $O_2$. Its central frequency is 57.95 GHz and its weighting function peaks near 90 mb. Three SSU channels (SSU1, SSU2, SSU3) measure infrared radiation from molecular $CO_2$ in the neighborhood of 15 microns. Their weighting functions peak near 15, 5, and 1.5 mb, respectively. The half-amplitude thicknesses for the MSU and SSU weighting functions are roughly 8 km and 16 km, respectively.

The data used are in the format of daily 5 × 5 deg global grids. They are produced by the British Meteorological Office from the original polar-orbiting satellite measurements. Distance and time weighting were used in their data processing. The distance weighting is conical, being 1 for the observations right at the grid point and decreasing linearly to 0 for observations at or beyond 500 km from the grid point. The time weighting is similar, being 1 for observations made at the analysis time (1200 UTC) and decreasing linearly to 0 for observations made at or beyond ±12 h from the analysis time. Gridpoints which have no data assigned were filled by interpolation from neighboring grids points having valid data.

The brightness temperature Tb is obtained from the radiation data by the inverse Planck law.

To avoid the leakage of strong annual and semiannual power in the spectral analysis, we chose the length of our data record to be exactly 4 years (from 1 April 1980 through 31 March 1984). Sharp spectral peaks at annual and semiannual oscillations were obtained in our results, confirming that there is little direct leakage (due to the finite length time series analyzed) of these oscillations to other frequencies.

Before spectral analysis, the data were checked and obviously bad data were removed and data gaps were filled by linear interpolation. By using nonoverlapping 3-day means, the time series were shortened by a factor of 3. This saves computing time and memory, but does not appreciably affect the low-frequency signals of interest here.

Spatial filtering is also used, not only because the slow variations of interest here are expected to have large spatial scales (the short-scale features are of less importance for this study), but also because there is an instrumental "scan angle effect" in the tropics, with strong components in the neighborhood of zonal wavenumber 14 (Yu et al., 1983).

The brightness temperatures $\mathrm{Tb}(\phi, \lambda, t)$ were zonally Fourier analyzed, then reconstructed $\mathrm{Tb}(\phi, \lambda, t)$ were obtained by using zonal wavenumbers 0 to 10. Here $\phi$ and $\lambda$ are latitude and longitude, respectively. The spatially filtered, 3-day mean brightness temperature $\mathrm{Tb}(\phi, \lambda, t)$ is analyzed by Fast Fourier Transformation technique:

$$\mathrm{Tb}(\phi, \lambda, t) = \sum_{n=0}^{244} [C_n(\phi, \lambda) \cos\omega_n t + S_n(\phi, \lambda) \sin\omega_n t]$$

$$= \sum_{n} \sum_{K=0}^{10} [C_c(\phi, K, \omega_n) \cos\omega_n t \cos K\lambda + C_s(\phi, K, \omega_n) \cos\omega_n t \sin K\lambda + S_c(\phi, K, \omega_n) \sin\omega_n t \cos K\lambda + S_s(\phi, K, \omega_n) \sin\omega_n t \sin K\lambda],$$

with

$$\omega_n = 2\pi n/(1464 \text{ day}).$$

$S_n(\phi, \lambda)$ and $C_n(\phi, \lambda)$ are Fourier coefficients of the local brightness temperature $\mathrm{Tb}(\phi, \lambda, t)$. All later calculations are based on these Fourier coefficients.

## 3. Results

### a. *Local Tb power spectra*

Using Fourier coefficients $S_n(\phi, \lambda)$ and $C_n(\phi, \lambda)$ the power spectrum of local brightness temperature is calculated:

$$P_n(\phi, \lambda) = [S_n^2(\phi, \lambda) + C_n^2(\phi, \lambda)]/2\Delta F,$$

with $\Delta F = (1464 \text{ day})^{-1}$. Here "local" means at a particular latitude $\phi$ and longitude $\lambda$. Balancing between good statistics and fine resolution, we chose a 5-point running mean in power spectra. Figure 1 shows several such spectra plotted in semilogarithmic coordinates. The confidence level scale shown in Fig. 1 is calculated from a posteriori statistics using the chi-square distribution. Details are given in the Appendix. The bandwidth (BW) scale shown in Fig. 1 is based on a 5-point running spectral mean.

The spectra shown in Fig. 1 suggest two separate spectral peaks in the low-frequency range (30–90 days), with periods of about 40–50 days and 55–65 days, respectively. The gridpoint (5°S, 175°W) is close to Canton Island (3°S, 172°W) where Madden and Julian (1971) first found the 40–50 day oscillation in the zonal wind and surface pressure. The Tb spectrum for this grid point shows a clear peak at 40–50 days (Fig. 1, bottom trace).

This period is in agreement with Madden and Julian's first report in 1971, although channel MSU4 is sensitive to the temperature of the lower stratosphere. The confidence level for the existence of 40–50 day oscillation at this gridpoint is higher than 95%, which is statistically significant when looking for a spectrum peak in a definite spectral and geographical region.

There are also suggestions of spectral features at both shorter (30–35 days) as well as longer periods (100–150 days) in Fig. 1. While various authors have discussed possible spectral peaks in the 1-month range, the possible long period feature (100–150 days) will require additional study. This is particularly true in light of the tendency of atmospheric spectra to exhibit increasing variance with decreasing frequency ("red" noise). In conjunction with the long-period feature, it is important to note that the annual oscillation and up to its fourth harmonic were replaced by the averages of their two neighboring spectral points, before performing the 5-point running mean in Fig. 1.

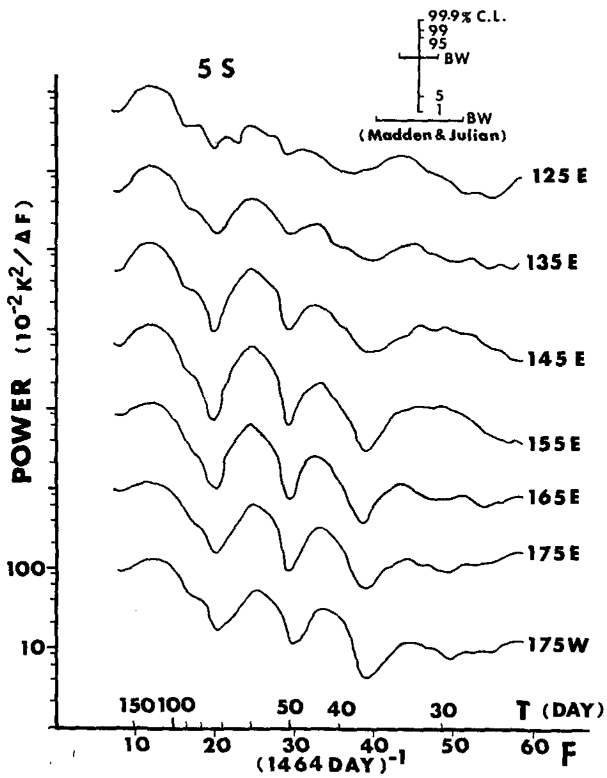


FIG. 1. Analyses of Microwave Sounder Unit channel 4 (MSU4) brightness temperature data representative of 30–150 mb atmospheric temperatures (weighting function peak near 90 mb): Power spectra vs frequency ($F$) of local brightness temperature Tb at 5°S latitude, for various longitudes from 125°E to 175°W. The spectra have been smoothed with five-point running means. The C.L. scale is based on the chi-square distribution. The statistical significance is discussed in the Appendix. Bandwidths (BW) for the present study as well as for those of Madden and Julian (1971) are shown. The power scale is correct for the lowest curve. Succeeding curves are displaced by ×10 for clarity. $\Delta F = (1464 \text{ day})^{-1}$.

### b. *Comparison of the 40–50 day and 55–65 day fluctuations*

Recent papers have suggested that low-frequency atmospheric spectra may be described as a broad band of 30–60 day, or even 30–90 day periods (Weickmann, 1981, 1983; Lau and Chan, 1985). Our results in Figs. 1 and 2 suggest that there may be sub-band features within the broader band. We here compare the 40–50 day and 55–65 day band spectral features from several aspects.

#### 1) Spatial distribution

To investigate the spatial distributions of the 40–50 day and 55–65 day fluctuations, confidence levels were calculated at every grid point. The confidence levels indicate whether the oscillations exhibit significant strength compared with the estimated background "noise."

In the Appendix, estimates are made of confidence levels based on both a priori and a posteriori statistics. To ensure that there is only one chance in 20 of sampling variations causing a spectral peak, the parameters of our analyses require 95% confidence levels (C.L.) for the a priori case, viz., in which a feature has been previously reported in a specified spectral band and geographical region. As reviewed in the Introduction, many investigators have reported features in a broad band of periods from about 1 to 2 months over the tropical Indian Ocean and tropical Pacific. Our results show statistically significant signals in the 40–50 day band near 5°S, 180°W (95% C.L.).

For regions in which previous investigations have not reported well-established low-frequency oscillations, a posteriori statistics must be utilized. In this case, ensuring that sampling fluctuations contribute at or below the 5% level requires 99.8% C.L. (see the Appendix).

The 40–50 day feature near 35°S, 100°W does meet the a posteriori statistics required for this band of periods, 99.9% C.L. (see the Appendix). This geographical region has not been generally recognized in connection with low frequency oscillations. The local Tb spectra of this region show clear evidence for the 40–50 day oscillation. Figure 3 shows spectra for several locations in this region. Note the strong 40–50 day peaks at 35°S, 105°W and 95°W. In this region, the signal of the 40–50 day oscillation can be traced into the upper stratosphere, as will be discussed shortly.

Concerning the lack of earlier reports of low frequency oscillations in the southeast Pacific, it should be noted that previous rawinsonde investigations did

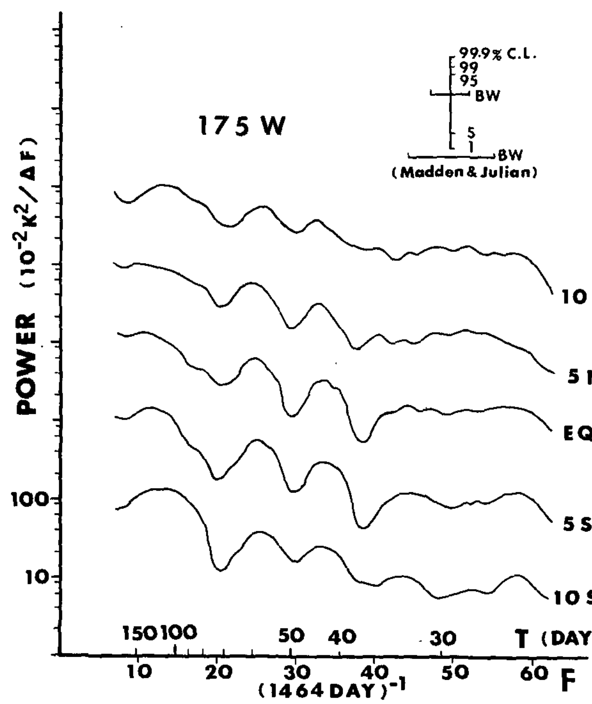


FIG. 2. As in Fig. 1, except spectra of local Tb at 175°W longitude, for various latitudes from 10°N to 10°S.

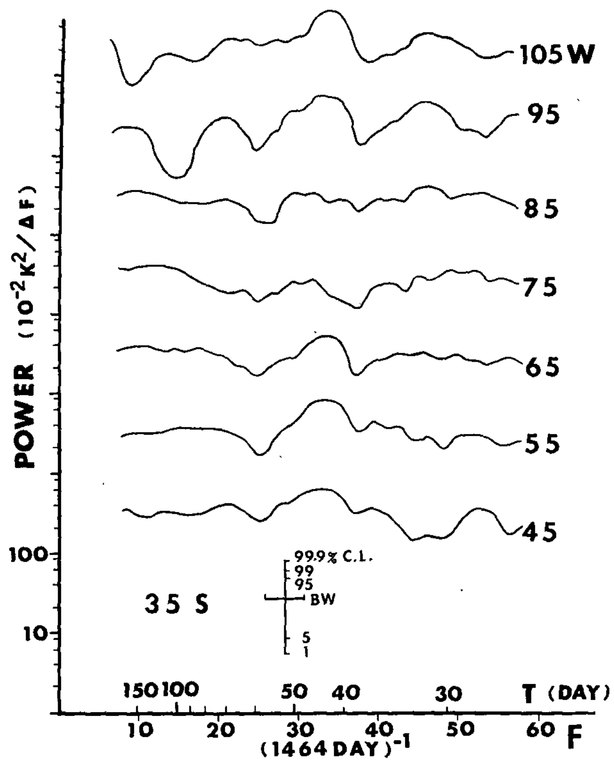


FIG. 3. Spectra of local MSU4 Tb as in Fig. 1, but for 35°S, at various longitudes from 105°W to 45°W.

not report analyses in this region. Moreover, the extensively used outgoing longwave radiation (OLR) data set contains implicit biases for regions in which high-level cloudiness is suppressed on a broad scale. This is the case for the southeast Pacific which is well known for its large-scale atmospheric subsidence. Satellite infrared cloud photos typically show few high-level clouds in this area. Thus OLR analyses are not as reliable over this region and rawinsonde analyses have not been previously reported.

We believe that 40–50 day oscillation in the southeast Pacific to be real. This is supported by the high confidence level we observe which passes the rigorous a posteriori statistic test. Moreover, and of considerable importance, there is recent corroboration of 40–50 day oscillations from analyses of an entirely independent data set, that of Easter Island (27°S, 109°W) rawinsonde measurements (Graves and Stanford, 1987). In the next section, it will be seen that these features are anticorrelated with the fluctuations in the central Pacific and may originate in the central Pacific or farther west.

The 55–65 day oscillation does not show a statistically significant signal in the southeast Pacific.

### 2) ZONAL WAVE COMPONENTS

Our zonal Fourier analyses indicate that the band of 55–65 day fluctuations is dominated by zonal wavenumber zero. Figure 4 shows the zonal mean (wavenumber zero) Tb spectra for low latitudes. The 55–65 day peak is evident for latitudes between 10°N and 10°S. But the 40–50 day peak, seen in the local Tb spectra for the central Pacific region (Fig. 1) is difficult to find in these zonal mean Tb spectra. Table 1 shows the zonal averaged variances contributed by different zonal wavenumber $K$:

$$\sigma_{\Delta\omega}(\phi, K) = \delta_K \sum_{\Delta\omega} [C_c^2(\phi, K, \omega_n) + C_s^2(\phi, K, \omega_n) + S_c^2(\phi, K, \omega_n) + S_s^2(\phi, K, \omega_n)],$$

$$\delta_K = \begin{cases} 1/2, & K = 0 \\ 1/4, & K \neq 0. \end{cases}$$

Here, the $\Delta\omega$ indicates the frequency band used. In the tropics, the fluctuations in the 55–65 day band are mainly due to zonal wavenumber 0, with the other wavenumbers contributing less than 20% over 5°N–5°S. For the 40–50 day band, the fluctuations in wavenumber 1 and 2 in the tropics are almost as important as wavenumber 0. In the extratropics, wave 1 and 2 are more important than wave 0, for the 40–50 day oscillation.

The difference between the zonal wave spectra of these two-band fluctuations is also shown by band-pass filtered one-point correlation maps, Figs. 5a, b. To make comparison easier, both maps were made with the same reference point (Eq. 175°W) where the signals

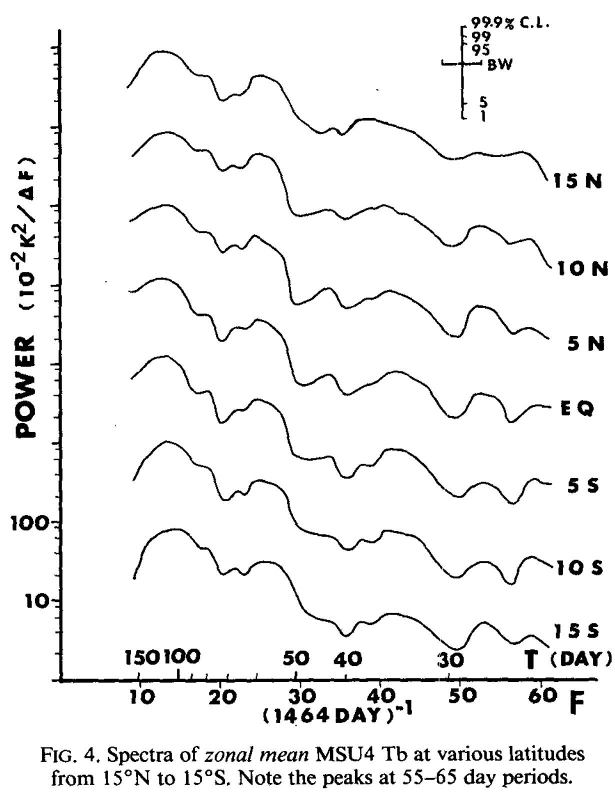


FIG. 4. Spectra of *zonal mean* MSU4 Tb at various latitudes from 15°N to 15°S. Note the peaks at 55–65 day periods.

TABLE 1. Percentage of zonally averaged variance of MSU4 brightness temperatures as a function of latitude and zonal wavenumber. Blank entries indicate values of less than 0.5%.

| Latitude | Zonal wavenumber | | | | | | | | | | |
|---|---|---|---|---|---|---|---|---|---|---|---|
| | 0 | 1 | 2 | 3 | 4 | 5 | 6 | 7 | 8 | 9 | 10 |
| *(a) Bandpassed fluctuations with periods of 39.0–51.4 days.* | | | | | | | | | | | |
| 40°N | 9 | 19 | 31 | 12 | 7 | 11 | 6 | 2 | 1 | 1 | |
| 30°N | 15 | 22 | 21 | 11 | 8 | 12 | 7 | 3 | 1 | 1 | |
| 20°N | 17 | 33 | 19 | 8 | 6 | 9 | 4 | 2 | 1 | 1 | |
| 10°N | 37 | 22 | 18 | 7 | 4 | 4 | 3 | 2 | 1 | 1 | 1 |
| Equator | 31 | 33 | 19 | 8 | 3 | 2 | 1 | 1 | | 1 | 1 |
| 10°S | 38 | 23 | 14 | 9 | 6 | 2 | 3 | 3 | 1 | 1 | 1 |
| 20°S | 6 | 37 | 16 | 15 | 8 | 4 | 8 | 3 | 2 | 1 | |
| 30°S | 5 | 29 | 22 | 12 | 14 | 8 | 5 | 2 | 1 | | |
| 40°S | 5 | 45 | 21 | 7 | 13 | 5 | 2 | | | | |
| *(b) Same as (a) but periods of 53.2–65.1 days.* | | | | | | | | | | | |
| 10°N | 74 | 12 | 4 | 3 | 3 | 2 | | | | | |
| 5°N | 81 | 9 | 4 | 2 | 2 | 1 | | | | | |
| Equator | 81 | 9 | 4 | 2 | 2 | 1 | | | | | |
| 5°S | 80 | 8 | 4 | 4 | 2 | 1 | | 1 | | | |
| 10°S | 62 | 18 | 7 | 7 | 2 | 2 | 1 | 1 | | | |

are strong in both bands. Here, 40–50 day and 55–65 day will be used to denote band-pass filtered analyses of 39.0–51.4 day and 53.2–65.1 day periods, respectively.

The correlation map for 55–65 day fluctuations (Fig. 5a) shows that the tropical regions around the entire earth are highly correlated with the central Pacific, with correlation coefficient of about 0.8. This is another indication, as noted previously in Table 1b, that the 55–65 day correlation is characterized predominately by zonal wave 0. The northern high latitudes are highly anticorrelated with the equatorial reference point, with correlation coefficients of about −0.6. There is another highly anticorrelated region centered near 65°S, 70°W in the Antarctic.

In contrast to the zonal wavenumber 0 domination of the 55–65 day correlation map, the correlation map for the 40–50 day fluctuation (Fig. 5b) indicates more zonal wavenumber 1 and 2 components. This is also consistent with Table 1a. In the 40–50 day map, there are two highly anticorrelated regions, located near 0° longitude, with latitudes of 35°N and 35°S. These midlatitude correlations are considered in more detail in a separate paper.

### 3) Phase variation

The correlation maps (Fig. 5a, b) of the band-pass filtered brightness temperatures reveal the tendency for the high latitudes to be out of phase with the tropics for the 55–65 day band fluctuations, while the 40–50 day oscillation near 5°S, 95°E tends to be out of phase with that at 5°S. This well-known Indonesia-central Pacific dipole structure is seen in the 40–50 day correlation map (Fig. 5b), even though the zonal means have not been removed. When the zonal mean is removed, the correlation coefficient between 95°E and 175°W along the equator becomes −0.7 (not shown here). The near 180° phase shift is in agreement with other authors' reports based on OLR data (Lau and Chan, 1985; Weickmann, 1983).

### 4) Temporal variation

To compare the temporal variations of the 40–50 and 55–65 day fluctuations, we calculated the band-pass-filtered local Tb time series. Figure 6a shows the 40–50 day band-pass filtered Tb for the region 5°S, 125°–175°E, and the region 35°S, 115–65°W. In the western tropical Pacific, the amplitude of the oscillation varies slowly with time, but does not show obvious seasonal variation (Fig. 6a). In contrast, in the southeast Pacific (Fig. 6b), clear seasonal variation in amplitude is evident, with a 1-yr modulation period being prominent. Note the change of scale in Fig. 6b, indicative of the strong southeast Pacific signal.

The 55–65 day band-pass-filtered local Tb time series at 5°S and 125–175°E are shown in Fig. 7. The western Pacific 55–65 day amplitude has smaller interannual variation than that of the 40–50 day oscillation. Comparing Figs. 6a and 7, it can be seen that the 40–50 day and 55–65 day oscillations were simultaneously strong in some regions, for example, 125–135°E during 1980–83. This is evidence against the hypothesis that these two oscillations are physically similar, having different frequencies due to variations in the basic state. Under such a hypothesis, they should not occur in the same region at the same time.

### 5) Middle and upper stratosphere

In order to get some information about low-frequency fluctuations in middle and upper stratosphere,

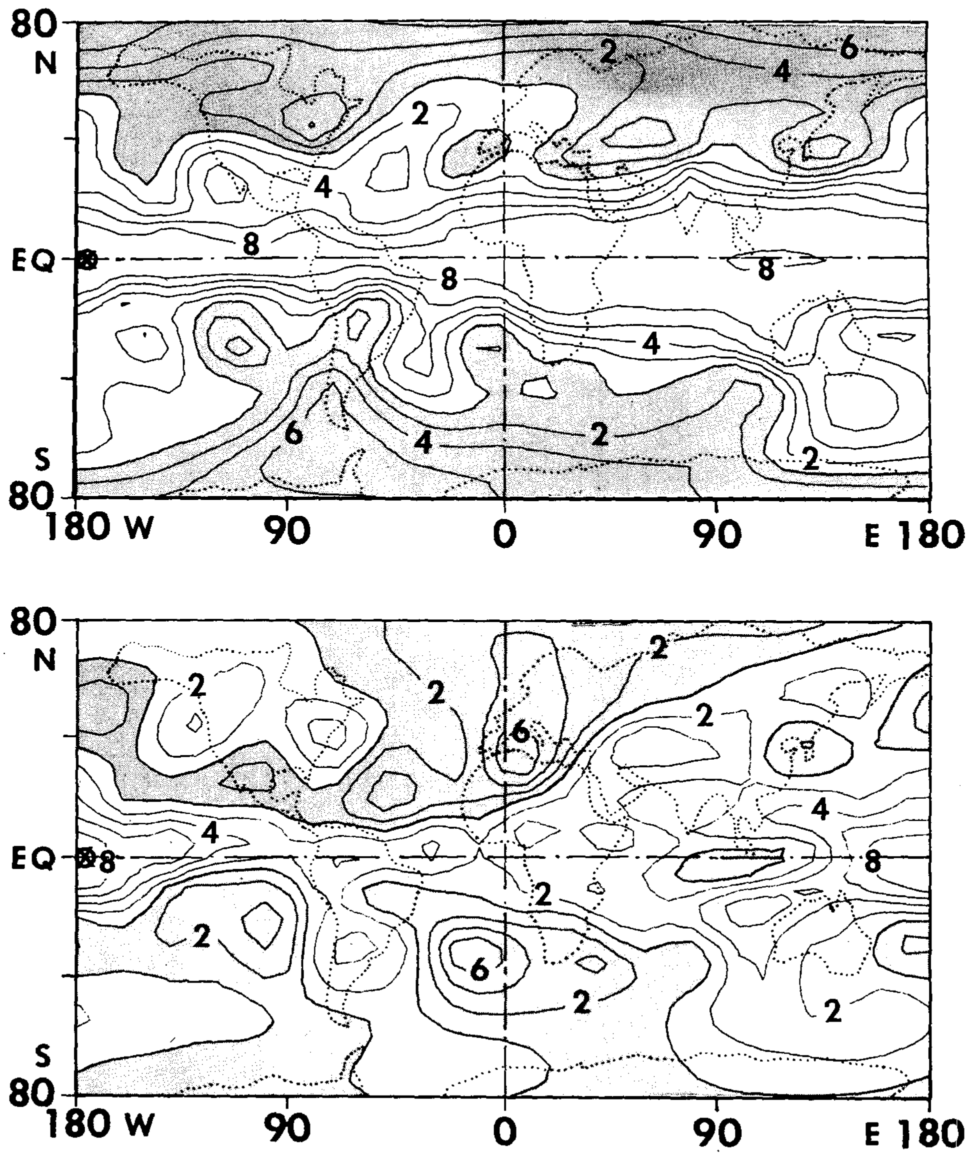


FIG. 5. (a) One point correlation map ($R \times 10$) for 55–65 day fluctuations with reference point indicated at equator, 175°W. For the parameters used here, the 95% confidence level is estimated to correspond to 0.52 (−0.52) for correlation (anticorrelation). (b) One point correlation map ($R \times 10$) for 40–50 day fluctuations with reference point indicated at equator, 175°W. For the parameters used here, the 95% confidence level is estimated to correspond to 0.40 (−0.40) for correlation (anticorrelation). The well-known dipole structure between Indonesia and the central Pacific is indicated weakly here. When the zonal mean is removed, the correlation between 95°E and 175°W along the equator becomes very strong, −0.7.

data from three SSU channels (SSU1, SSU2, SSU3) were analyzed. The analysis procedures were the same as used to analyze the MSU4 data. Figure 8 shows the C.L. for the 40–50 day oscillation for different altitude layers. The results indicate that the 40–50 day signal over the SE Pacific can be traced up to the upper stratosphere.

There is also a region of high confidence levels near 60°S latitude. This high C.L. area tilts westward with increasing altitude (Fig. 8). The reason for the strong 40–50 day oscillation in high southern latitudes is not known. The 55–65 day oscillations did not show any statistically significant regions in the mid- to upper stratosphere (SSU data) and are not shown here.

## 4. Summary and discussion

1) In the lower stratosphere, over the tropical Pacific, the spectra of local Tb show two separate peaks in the low-frequency range (30–90 day), with 40–50 day and 55–65 day periods. The 40–50 day oscillation is strong over the equatorial central Pacific, but not clearly seen

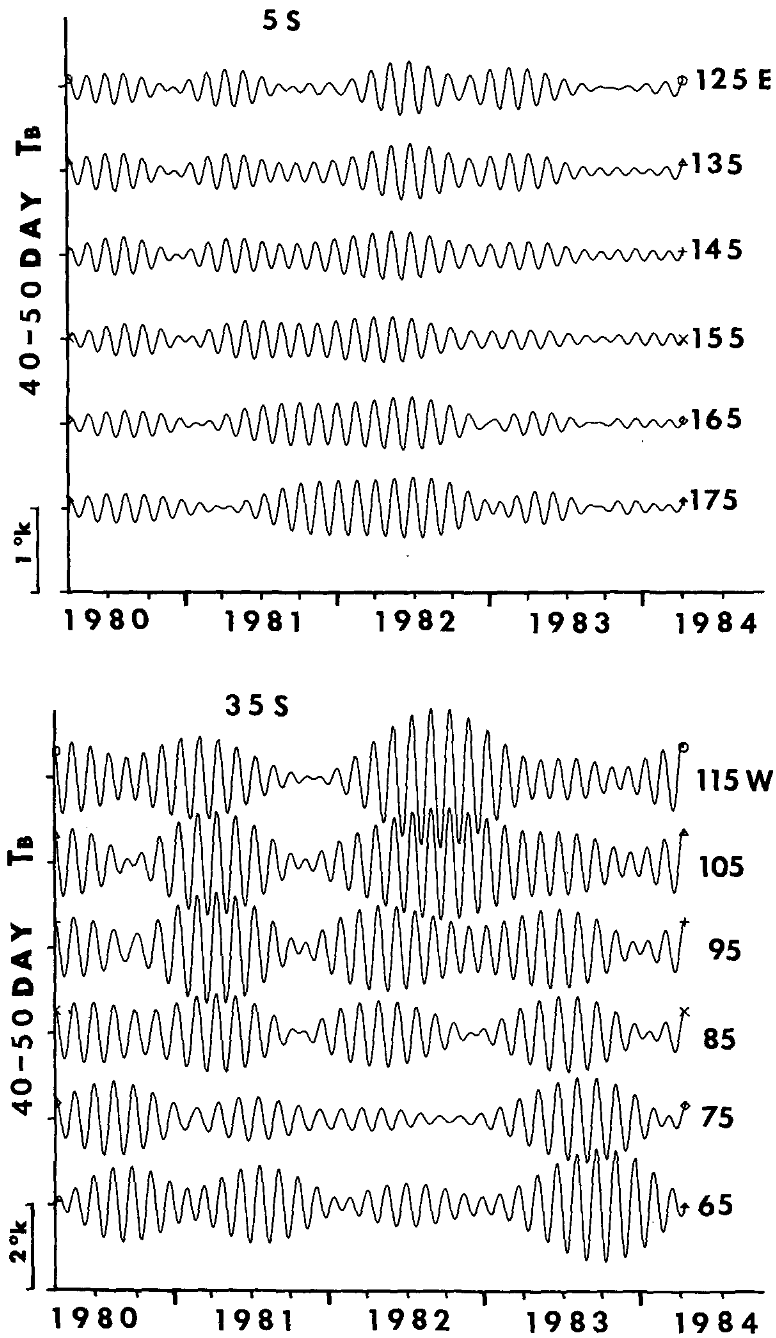


FIG. 6. (a) Bandpass filtered (39–51 day periods) MSU4 Tb time series at 5°S, for various longitudes from 125°E to 175°E. (b) As in (a), but at 35°S, for various longitudes from 115°W to 65°W. Note the change of amplitude scale, indicative of the strong signal in the southeast Pacific.

elsewhere in the tropics. The 55–65 day oscillation is observed all over the tropics and is dominated by zonal wavenumber 0.

2) The 40–50 day oscillation is also observed over the southeast Pacific, from the lower through the upper stratosphere. In southern high latitudes (near 60°S), there is a large region having such oscillations in the southern winter.

3) The results presented here suggest that there may be more than one physical mechanism which contributes to the low frequency oscillations:

(i) *Lower stratosphere* (Fig. 5): The 55–65 day fluctuations are dominated by zonal wavenumber 0 in the tropics, and are anticorrelated with polar latitudes. The northern polar signal is generally

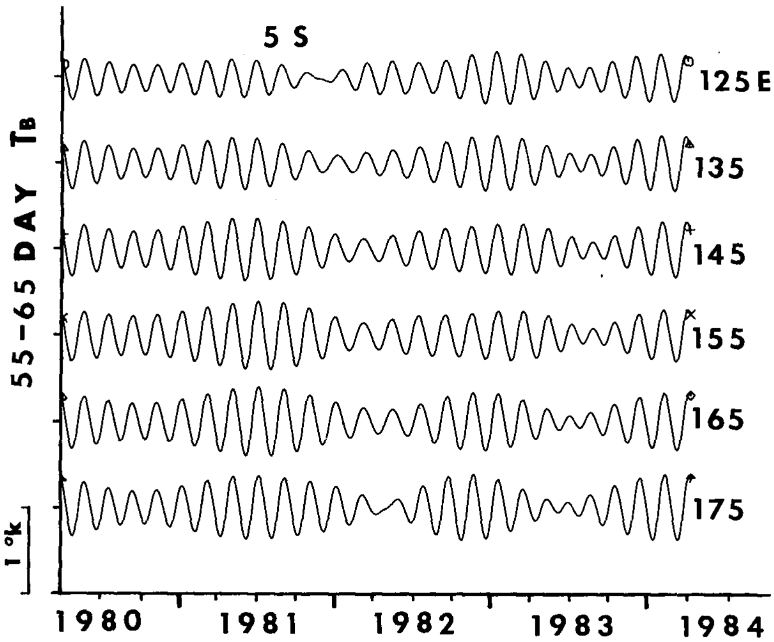


FIG. 7. As in Fig. 6a, but with filter window of 53.2–65.1 day periods.

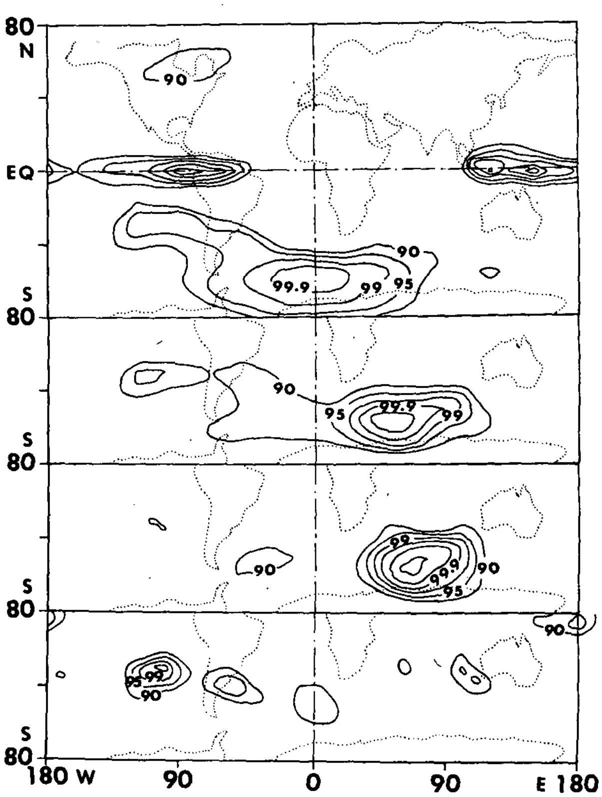


FIG. 8. Confidence level maps for 40–50 day oscillations in three SSU infrared stratospheric channels and one MSU channel (MSU4). The 90, 95, 99 and 99.9% C.L.'s are indicated. The 99.9% C.L. is statistically significant at the a posteriori level in these analyses. Top to bottom: weighting function peaks near 1.5, 5, 15, 90 mb, respectively.

strongest in winter and nearly out of phase with the tropics. In contrast, the 40–50 day signal exhibits strongest power at zonal wavenumbers 1 and 2, and is not correlated with polar latitudes.

(ii) *Middle and upper stratosphere* (Fig. 8): The 40–50 day signal exists in the middle and upper stratosphere over high southern latitudes, and is also evident in the tropical upper stratosphere (although there the amplitude is weak). This contrasts with the 55–65 day fluctuations which are not observed above the lower stratosphere in our analyses.

4) The results presented here reveal strong 40–50 day fluctuations in the southeast Pacific, a region not generally recognized in other low-frequency investigations. [A possible exception is Quay (1984) who recently reported on 30–50 day tropospheric oscillations. One of his spectral plots is for the west edge of the southeast Pacific region in question. Krishnamurti and Gadgil (1985) also find low-frequency signals near this southeast Pacific region.] The reason that the southeast Pacific has been overlooked appears to be that previous rawinsonde analyses have not used southeast Pacific stations (indeed they are almost nonexistent except for Easter Island) and OLR analyses are biased against regions with little high cloudiness, such as the southeast Pacific with its general sinking air motions. However, recent analyses of rawinsonde data for Easter Island (27°S, 109°W) have corroborated the existence of 40–50 day oscillations in the southeast Pacific (Graves and Stanford, 1987). The 40–50 day oscillation over the

southeast Pacific (35°S) exhibits a clear seasonal variation (Fig. 6b).

Further observational studies are needed to better quantify the low-frequency phenomenon as well as provide guidance for theoretical work, especially at high latitudes and in the stratosphere.

*Acknowledgments.* This material is based upon work supported jointly by the National Science Foundation and the National Aeronautics and Space Administration under grants ATM 8402901 and 8603943. We especially appreciate helpful discussions on computing with Mr. L. R. Lait and statistics with Mr. C. E. Graves. We also thank two anonymous referees whose perceptive criticism stimulated significant improvement in the results and manuscript.

## APPENDIX

## Confidence Level Determination

### 1. Peaks in local (specific location) spectra

Using the a posteriori statistical argument discussed by Madden and Julian (1971) for our analysis case, there is only 1 chance in 20 that any spectral peak will rise more than the 99.9% confidence level above the local background in our spectrum. This is based on our use of a time series of 488 points (covering a 4-yr period with 3-day means) and, further, using five-point running spectral averages in the power spectrum. With 244 spectral points from FFT analysis, the five-point running means yield effectively about 49 degrees of freedom. At the 99.9% confidence level, if 20 such 4-yr spectra were obtained, in only 1 of these spectra would it be expected that a random peak would be found to be at or higher than the 99.9% C.L. above the estimated nearby background level.

In calculating the confidence level, we estimated the background level in the following way: The annual, semiannual, third and fourth harmonics of the annual oscillation were removed and replaced by the averages of their two adjacent spectral power points. We then fitted 47 spectral points [from 7 to 53 $(1464\ \text{day})^{-1}$ on the frequency scale in Fig. 1], centered at about the 50-day period, with a quadratic background by using least square fitting. This is a conservative estimate, in that, if the two peaks are true signals, the background estimated including them will be too high.

We suggest, then, that spectral features rising to the 99.9% confidence level may be considered statistically significant in our spectral analyses, even though they have not been previously reported in local spectra analyses (a posteriori statistics). On the other hand, previously reported features are here considered to be statistically significant when they reach the 95% confidence level for the geographical region where they have been previously reported (a priori statistics).

### 2. Significance of spectral peaks on a geographical grid

Consider a spectral peak which reaches the $X\%$ confidence level in some arbitrarily chosen spectral interval (say, the 40–50 or 55–65 day peak). If this is a randomly occurring peak, it has a probability of $1-X\%$ of being found in the arbitrarily chosen spectral interval. Suppose there are $N$ degrees of freedom in the horizontal (global) distribution of the variable in question. Then, by the binomial distribution, there will be a probability of $(X\%)^N$ of not finding such a peak in any geographical region from whole globe.

If, now, one finds such a peak in the chosen spectral interval, and in at least one geographical region of the grid, there will be only 1 chance in 20 that the result is due to sampling fluctuations, provided it is required that

$$1-(X\%)^N = 5\%. \tag{B1}$$

If $N$ can be estimated by some technique, the required confidence level $X\%$ is then easily obtained from

$$X\% = \sqrt[N]{95\%}. \tag{B2}$$

A rigorous estimate of $N$ can be obtained, for example, by Monte Carlo techniques (Livezey and Chen, 1983), although the amount of computing required can be significant.

In the present analysis, we obtain a less rigorous but still useful estimate of $N$ by an alternate method. We have noted (Table 1) that about 90% of the variation in the 55–65 day fluctuations is contained in zonal wavenumbers 0, 1, 2, and 3. The number of degrees of freedom in the zonal direction can then be estimated as approximately 7 (1 for wavenumber 0, and 1 for each of the sine and cosine independent variables of wavenumbers 1, 2, and 3). This may be a conservative estimate of $N$, due to the very uneven weighting of zonal wavenumbers in the variations. To estimate the degrees of freedom for the latitudinal direction, experience suggests that large-scale motions in the atmosphere usually have latitudinal scales comparable with their zonal scales. In the latitudinal direction, the number of degrees of freedom is estimated as $\sim 7/2$, since the pole-to-pole angular distance is half that in the zonal direction. Thus, an estimate can be given for the global degrees of freedom as $N \sim 7 \times 7/2$. This allows an estimate of the least confidence level $X\%$ to be used in deciding if the 55–65 day spectral peak observed on our geographical grid is due to random sampling effects: $X \geq 99.8\%$.

Similarly, for the 40–50 day feature, Table 1 reveals that the variance is dominated by wavenumbers 0 to 5. Thus $N \sim 11 \times 11/2$, giving the requirement $X\% \geq 99.9\%$ for the 40–50 day peak.

*Note added in revision:* These estimates for $N$ have been corroborated by independent calculations based on Monte Carlo techniques and are discussed in a separate paper.

## REFERENCES


Anderson, J. R., and D. E. Stevens, 1987: The response of the tropical atmosphere to low-frequency forcing. *J. Atmos. Sci.*, **44**, 676–686.

——, D. E. Stevens and P. R. Julian, 1984: Temporal variations of the tropical 40–50 day oscillation. *Mon. Wea. Rev.*, **112**, 2431–2438.

Chang, C. P., 1977: Viscous internal gravity waves and low-frequency oscillations in the tropics. *J. Atmos. Sci.*, **24**, 901–910.

Goswami, B. N., and J. Shukla, 1984: Quasi-periodic oscillations in a symmetric general circulation model. *J. Atmos. Sci.*, **41**, 20–37.

Graves, C. E., and J. L. Stanford, 1987: Low-frequency atmospheric oscillations over the southeast Pacific. *J. Atmos. Sci.*, **44**, 260–264.

Krishnamurti, T. N., and S. Gadgil, 1985: On the structure of the 30–50 day mode over the globe during FGGE. *Tellus*, **37A**, 336–360.

Lau, K. M., and P. H. Chan, 1985: Aspects of the 40–50 day oscillation during the northern winter as inferred from outgoing longwave radiation. *Mon. Wea. Rev.*, **113**, 1889–1909.

Livezey, R. E., and W. Y. Chen, 1983: Statistical field significance and its determination by Monte Carlo techniques. *Mon. Wea. Rev.*, **111**, 46–59.

Madden, R. A., and P. R. Julian, 1971: Detection of a 40–50 day oscillation in the zonal wind in the tropical Pacific. *J. Atmos. Sci.*, **28**, 702–708.

——, and ——, 1972: Description of global-scale circulation cells in the tropics with a 40–50 day period. *J. Atmos. Sci.*, **29**, 1109–1123.

Murakami, T., T. Nakazawa and J.-H. He, 1984: On the 40–50 day oscillations during the 1979 northern hemisphere summer. Part I: Phase propagation. *J. Meteor. Japan*, **62**, 440–468.

——, —— and ——, 1984: On the 40–50 day oscillations during the 1979 northern hemisphere summer. Part II. Heat and moisture budget. *J. Meteor. Japan*, **62**, 469–484.

Quah, L. C., 1984: On the 30–50 day troposphere oscillation during the 1978–1979 northern winter. *J. Meteor. Soc. Japan*, **62**, 261–272.

Webster, P. J., 1983: Mechanisms of monsoon low-frequency variability: Surface hydrological effects. *J. Atmos. Sci.*, **40**, 2110–2124.

Weickmann, K. M., 1982: Intraseasonal fluctuations in near-global-scale modes of circulation and outgoing longwave radiation during Northern Hemisphere winter. Ph.D. thesis, University of Wisconsin, Madison, 107 pp.

——, 1983: Intraseasonal circulation and outgoing longway radiation modes during Northern Hemisphere winter. *Mon. Wea. Rev.*, **111**, 1838–1858.

——, G. R. Lussky and J. E. Kutzbach, 1985: Intraseasonal (30–60 day) fluctuations of outgoing longwave radiation and 250 mb stream function during northern winter. *Mon. Wea. Rev.*, **113**, 941–961.

Yamagata, T., and Y. Hayashi, 1984: A simple diagnostic model for the 30–50 day oscillation in the tropics. *J. Meteor. Soc. Japan*, **62**, 709–717.

Yu, W.-B., and J. L. Stanford, 1984: Stratospheric circulation in the southern summer/northern winter 1980–1981: Behavior of zonal waves 1–10. *J. Atmos. Sci.*, **41**, 2179–2188.